

## Supplementary Information

### Functional analysis of rare anti-Müllerian hormone protein-altering variants identified in women with PCOS

L. Meng, A. McLuskey, A. Dunaif, J.A. Visser

#### Contents

**Supplementary Table S1** Circulating AMH levels in individual carriers of six AMH variants that we did not functionally analyze.

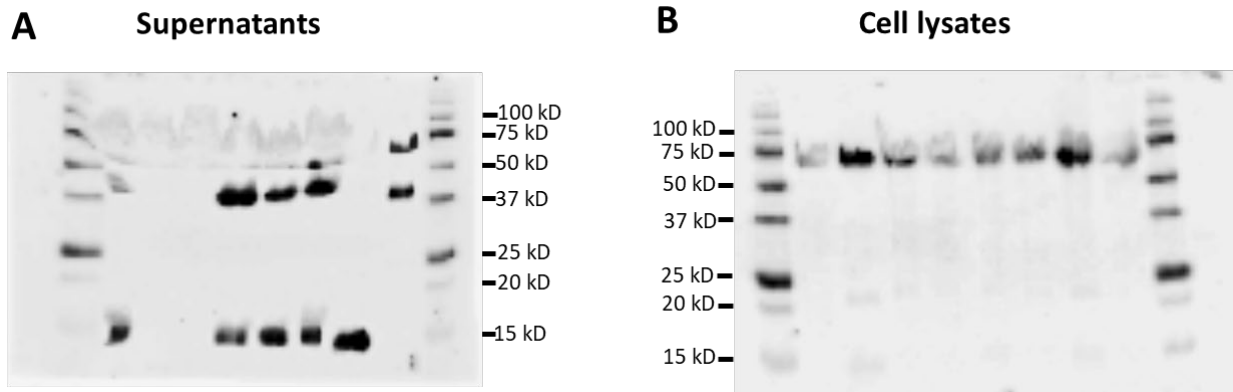
**Supplementary Figure S1** Uncropped western blots of AMH variants in HEK293 cells.

**Supplementary Figure S2** Colocalization of wt-hAMH, hAMH-<sup>352</sup>S, hAMH-<sup>151</sup>S and hAMH-<sup>506</sup>Q in stably transfected human embryonic kidney epithelial HEK293 cells.

**Supplementary Table SI Circulating AMH levels in individual carriers of six AMH variants that we did not functionally analyze.**

| <b>Variants</b> | <b>A24T</b> | <b>P46A</b> | <b>T99S</b> | <b>R302Q</b> | <b>P366L</b> | <b>Splicing<br/>(ex2/3)</b> |
|-----------------|-------------|-------------|-------------|--------------|--------------|-----------------------------|
| AMH, ng/mL*     | 9.43        | 3.49        | 12.23       | 5.99         | 27.52        | 7.43                        |
| AMH, ng/mL#     | 7.89        | 2.94        | 10.56       | 4.87         | 21.38        | 6.04                        |

Measurement of serum AMH by \* picoAMH assay (Ansh Labs) or # Lumipulse G1200 (Fujirebio).

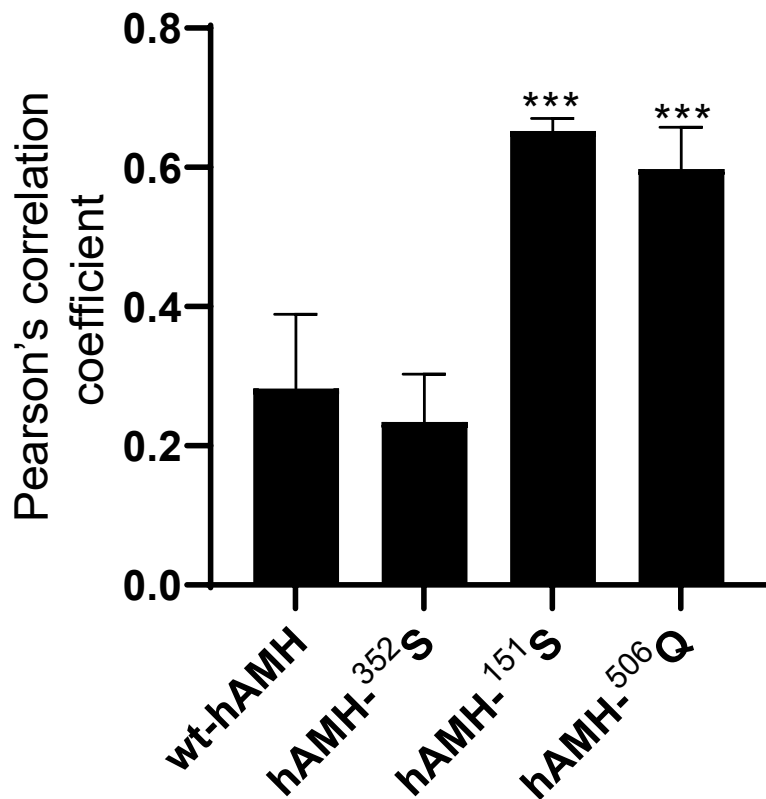


**Supplementary Figure S1. Uncropped western blots of AMH variants in HEK293 cells.**

Western blot analysis of AMH variants: full uncropped blots of Figure 4.

Western blot analysis of the human embryonic kidney epithelial HEK293 cells stably expressing the anti-Müllerian hormone (AMH) variants with the wild-type cleavage site RAQR or the inactive cleavage site RAGA. The mature region-specific 5/6A antibody recognizes the AMH precursor protein (~75 kD), the cleaved C-terminal mature protein (~15 kD) and a second subunit owing to a possible second cleavage site (~40 kDa). The relative molecular masses (kD) of the protein marker are indicated. Supernatants **(A)**

Full uncropped blot of Figure 4A. Lane 1: wt-hAMH-RAQR; lane 2: hAMH-<sup>151</sup>S; lane 3: hAMH-<sup>506</sup>Q; lane 4: hAMH-<sup>352</sup>S; lane 5: hAMH-<sup>362</sup>S; lane 6: hAMH-<sup>519</sup>V; lane 7: wt-hAMH-RARR; lane 8: wt-hAMH-RAGA. Cell lysates **(B)** Full uncropped blot of Figure 4B. Lane 1: wt-hAMH-RAQR; lane 2: hAMH-<sup>151</sup>S; lane 3: hAMH-<sup>506</sup>Q; lane 4: hAMH-<sup>352</sup>S; lane 5: hAMH-<sup>362</sup>S; lane 6: hAMH-<sup>519</sup>V; lane 7: wt-hAMH-RARR; lane 8: wt-hAMH-RAGA.



**Supplementary Figure S2. Colocalization of wt-hAMH, hAMH-<sup>352</sup>S, hAMH-<sup>151</sup>S and hAMH-<sup>506</sup>Q in stably transfected human embryonic kidney epithelial HEK293 cells.**

Colocalization of wt-hAMH, hAMH-<sup>352</sup>S, hAMH-<sup>151</sup>S and hAMH-<sup>506</sup>Q in stably transfected human embryonic kidney epithelial HEK293 cells with endoplasmic reticulum was analyzed by double immunofluorescent staining (confocal microscopy) and measured by Pearson's correlation coefficient (N=6). Statistical differences were analyzed by one-way ANOVA parametric test with Dunnett multi-comparison using the Prism 9 Software; \*\*\*P < 0.001